JACS
JOURNAL OF THE AMERICAN CHEMICAL SOCIETY

ARTICLE

pubs.acs.org/JACS

Folding of a Salivary Intrinsically Disordered Protein upon Binding to Tannins

Francis Canon,[†] Renaud Ballivian,[†,‡] Fabien Chirot,[‡] Rodolphe Antoine,[§] Pascale Sarni-Manchado,[†] Jérôme Lemoine,[‡] and Philippe Dugourd*[,§]

[†]INRA, UMR1083 Science Pour l'Oenologie, Polyphenol Interaction, Bât 28, 2 place Viala F-34060 Montpellier, France

[‡]Université de Lyon, F-69622, Lyon, France

[§]Université Lyon 1, F-69622, Villeurbanne; CNRS, F-69622, Lyon, France

Supporting Information

ABSTRACT: We used ion mobility spectrometry to explore conformational adaptability of intrinsically disordered proteins bound to their targets in complex mixtures. We investigated the interactions between a human salivary proline-rich protein IB5 and a model of wine and tea tannin: epigallocatechin gallate (EgCG). Collisional cross sections of naked IB5 and IB5 complexed with $N = 1-15$ tannins were recorded. The data demonstrate that IB5 undergoes an unfolded to folded structural transition upon binding with EgCG.

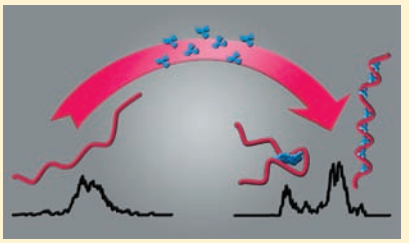

INTRODUCTION

The basic concept regarding the activity of proteins was dominated by the view that proteins need to have a well-defined three-dimensional structure for their function. However, during the past decade this view has changed,[1,2] and the sequence-to-structure-to-function paradigm had to be reassessed. Numerous proteins do have a well-defined function that requires intrinsic disorder, and the term of intrinsically disordered protein (IDP) has been proposed to describe this group.[1,3−5] IDPs appear to be rather common in living organisms especially in higher eukaryotes: primary sequence analyses indicate that about 10−20% of full-length proteins belong to this class and that 25−40% of all residues fall into such regions. The intrinsic lack of structure can confer functional advantages like the ability to bind several and/or different ligands. Moreover, many IDPs undergo coupled binding and folding processes that are intrinsically related to their dedicated function.[1−3] Now, the ability of IDPs to bind several ligands and in some cases to aggregate in large supramolecular edifices leads to mixtures of complexes with different stoichiometries and heterogeneous conformations. While several strategies are emerging for the characterization of flexible proteins, the study of mixed IDP−target complexes and of their assembly processes is highly challenging and requires new approaches. Besides heteronuclear multidimensional NMR[4,6] and small angle diffraction techniques[7,8] that are now used for IDPs, spectroscopy was used to get structural information on binding of tannins to proteins and spin relaxation measurements to get insight into molecular dynamics of the complexes.[9,10] Mass spectrometry combined to ion mobility (IMS) has the great advantage to allow determination of complex distributions and the qualitative structure of each of the species.[11−13] While much of the early IMS work on protein unfolding was performed using denaturing conditions,[14] measurements following electrospray ionization from "native" conditions support the use of ion mobility-mass spectrometry as a tool for structural biology.[15,16] For example, this method was recently applied with success to study the aggregation of a number of the amyloid-beta protein isoforms of A beta 40 and A beta 42,[17,18] prion,[19] and of α-synuclein proteins,[20] which are IDPs involved in several neurodegenerative diseases. Here, we explore the potentiality of IMS to study the structure of IDPs bound to their targets.

We investigated the interactions between the human salivary proline rich protein IB5 and a model of wine and tea tannin: epigallocatechin gallate (EgCG) (IB5 sequence and chemical structure of EgCG are given in the Supporting Information).[21,8] Tannins are phenolic compounds ubiquitous in plant and plant-based food.[22] The major part of plant/fruit tannins occurs through condensed forms. These condensed tannins continuously rearrange, polymerize, and break. They undergo different intra- and intermolecular reactions, among which oxidation reactions are the most important[23] and, through nucleation and growth processes, they can form colloidal particles.[24] They bind efficiently to salivary proline-rich proteins (PRPs) and thereby form soluble and nonsoluble tannin protein complexes.[25−27] These properties are considered to be responsible for astringency.[28,29] From a biological point of view, tannins act as protecting molecules toward herbivore species. This role has been attributed to their ability to interact with proteins, to precipitate them, and to inhibit gastrointestinal enzymes thereby reducing the digestibility of plant proteins.[30]

Received: January 19, 2011
Published: April 27, 2011

IB5 is a human protein which only known function is to bind and to scavenge tannins. Structurally speaking, IB5 belongs to the extendedly disordered family characterized by low sequence complexity and peculiar hydrodynamic dimensions.[4,31] Indeed, IB5 has a hydrodynamic dimension typical of considerably extended polypeptide chain and does not possess any ordered secondary structures.[32] The involvement of PRPs in the adaptation to a tannin diet as an astringency mediator and as a scavenger is related to their ability to establish noncovalent interactions with tannins. High tannin concentrations lead to insoluble IB5−tannin complexes, whereas lower ones give rise to soluble tannin−IB5 complexes with several stoichiometries.[27,33] These data suggest different recruitment schemes of binding partners related to conformational variability and adaptability. In the present work, ion mobility experiments show an unfolded to folded transition of IB5 protein induced by tannin binding.

MATERIALS AND METHODS

Epigallocatechin gallate (EgCG) was purchased from Sigma (Sigma Chemical Co., Poole, Dorset, U.K.). The IB5 human salivary proline rich protein was produced by the use of the yeast *Pischia pastoris* as a host organism and purified as previously described.[33] EgCG and protein stock solutions were prepared in the following medium: water/ethanol, 88:12 (v/v) acidified to pH 3.2 with acetic acid, which corresponds to the mouth conditions in the presence of red wine. IMS spectra were obtained with a home-built ESI ion mobility mass spectrometer.[34] Electrosprayed ions enter the instrument through a heated capillary interface held at 473 K and are accumulated in a small cylindrical ion trap.[35] Ion packets are periodically injected into a one meter long drift cell containing ≈10 Torr of He and travel through the influence of a uniform electric field (E = 770 V m^{-1}). At the exit of the cell, species are separated in drift-time according to their diffusion cross section. Compact ions display shorter drift-times than ions with extended structures. Then, the ions go through a quadrupole and a collision cell and are accelerated into a perpendicular reflectron time-of-flight mass spectrometer. 2-D maps (drift time, m/z) are recorded.

The ion mobility K is given by (eq 1):

$$t_d = \frac{L}{KE} \quad (1)$$

where L is the length of the drift cell, E is the electric field value in the cell, and t_d is the drift time across the cell. The ion mobility resolution of our instrument is ∼50. The experimental uncertainties on the determined K values are estimated to be 1%.

The mobility is related to the averaged collision cross section Ω_{avg} of the ion and buffer gas atom via eq 2:[36]

$$K = \frac{3}{16}\frac{ze}{N}\left(\frac{1}{m}+\frac{1}{M}\right)^{1/2}\left(\frac{2\pi}{kT}\right)^{1/2}\frac{1}{\Omega_{avg}} \quad (2)$$

where T is the temperature, ze the charge on the ion, N the buffer gas number density, and m and M, the masses of the neutral atom and ion, respectively .

Circular dichroism (CD) spectra were recorded on a Chirascan circular dichroism spectrometer (Applied Photophysics Ltd., Leatherhead, U.K.) using a 0.5 mm path length cell and analyzed with the CDtool software (Birkbeck College, London, U.K.).[37] The spectra of pure EgCG solutions at the desired concentration were subtracted from those of IB5:N EgCG to obtain the CD spectrum of the complexed protein.

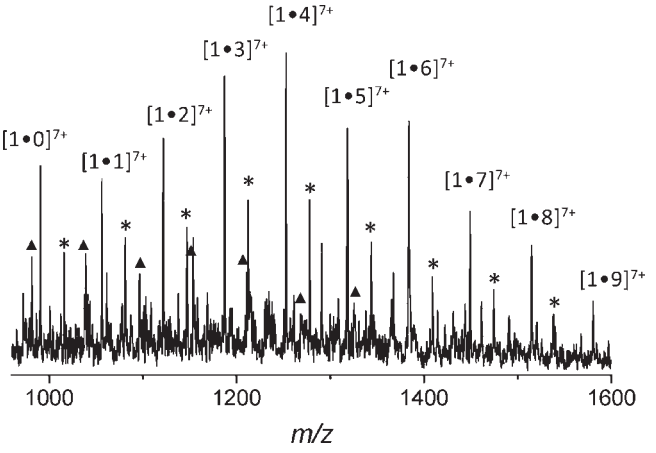

Figure 1. Positive ion mass spectrum of 1:20 IB5/EgCG (molar ratio) interaction mixture. Peaks for $[IB5a \cdot N\ EgCG]^{7+}$ are labeled. ▲ correspond to $[IB5a \cdot N\ EgCG]^{8+}$ complexes starting at N = 2. ∗ correspond to $[IB5b \cdot N\ EgCG]^{7+}$ complexes starting at N = 1.

RESULTS AND DISCUSSION

MS and IMS Data. The mass spectrum obtained by electrospraying the protein solution displayed a series of protonated peaks corresponding to three IB5 isoforms (a, 6923.70 Da; b, 6642.63 Da; and c, 6360.39 Da) with charge states ranging from 5+ to 10+ (see the Supporting Information, Figure S1). For interaction studies, IB5 and EgCG solutions were combined at a molar ratio of 1:20 (IB5/EgCG). Though crowded, the mass spectrum reveals free IB5 and IB5 supramolecular complexes with stoichiometries ranging from 1 up to 9 tannins (Figure 1). The abundance of the stoichiometries seems to follow a Poisson-like distribution. As a Poisson process is a stochastic process in which events occur continuously and independently of one another, this observation is in favor of a noncooperative sticking process.[38] The fragmentation spectrum (MS/MS) obtained after isolation and collision excitation of the supramolecular complex of IB5 with 9 tannins (charge state 7+) is shown in Figure S2 in the Supporting Information. The different fragment ions correspond to the free protein and complexes containing 1−8 tannins as well as the free tannin ion. It shows that the sequential loss of tannins is the preferred fragmentation pathway of the initial complex. The IMS contribution allows a study of the conformation of each complex and the resolution of eventual conformers. Figure 2 displays collisional cross sections of selected stoichiometries recorded for charge state 7+. For the naked protein, one broad peak is observed, which corresponds to a collision cross section centered at 1350 Å^2. The peak is much broader than what would be obtained from the diffusion equation assuming a single mobility,[13,36,39] which has to be correlated to the unstructured character of this type of proteins. Note that this value is, for example, much larger than the one (1050 Å^2) measured for the $(M + 7H)^{7+}$ ion of BPTI, a globular structured protein with a close molecular weight (M_w 6512 Da) used here as a standard. Binding of 1−7 EgCG ligands does not modify the general shape of the cross section profile. As expected, an increase in the collision cross section is observed as the number of bound ligands grows. The peaks are still broad in agreement with the expected non-specificity of protein−tannin interactions. From 10 ligands, a second feature appears in the collision cross section profile beside the one following the initial trend from the naked

protein. The two populations correspond to structural families that do not interconvert during the travel through the drift cell (drift time of ~60 ms). The second one is shifted to lower collisional cross section values (~1200 Å^2). Thereby, this new population corresponds to more compact conformations. Though the mass of IB5 complexed with 13 EgCG is twice the mass of the naked protein (12 877 Da versus 6 923 Da), the collision cross section of this more compact oligomer is smaller than the one of the protein. Interestingly, the cross section of the compact state increases little as the number of bound tannins grows, in contrast with the expended structures. The ratio of folded to unfolded states grows with the stoichiometry indicating the requirement of several tannins to stabilize the folded state. IMS results for charge states 6+ to 9+ are plotted in Figure 3. A transition was also observed for charge state 6+ and its onset for charge state 8+. The comparison of the results recorded for the different charge states shows that low charge states favor folded structures. This indicates that the role of the tannin molecules here is at least partially related to the screening of Coulombic forces that, in the gas phase, favor an elongated ensemble of conformations. High-charge state IB5 ions requires a larger amount of ligand molecules to convert down to the smaller structure. Though the structures may be stretched by Coulombic repulsion, the gas phase data presented here demonstrate that IB5 undergoes a structural transition upon binding with EgCG.

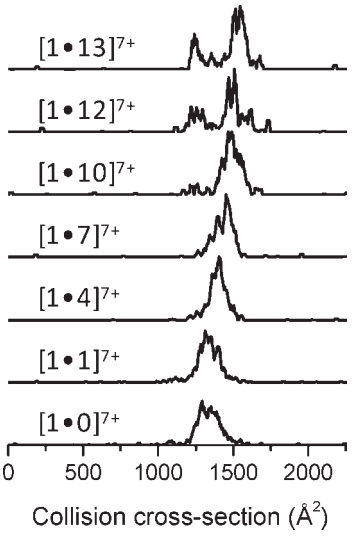

Figure 2. Collision cross section distributions for the 7+ charge state of IB5a and IB5a·*N* EgCG complexes (*N* = 0, 1, 4, 7, 10, 12, and 13).

Circular Dichroism. Circular dichroism (CD) experiments recorded on pure IB5 solution and on two 1:N IB5/EgCG (N = 10 and 40) mixtures further support the gas phase observation (Figure 4). The IB5 CD spectrum is characteristic of a wholly unfolded structure. An important modification of the CD curve shape of the protein occurs for N = 40 while for N = 10 the CD curve remains almost unchanged from the pure protein one. For 1:40 IB5/EgCG mixture, the band at 202 nm is red-shifted and the intensity of the band at 230 nm increases. These changes in the spectrum demonstrate a modification of the shape of the IB5 protein when involved in the complex in solution. The positive band that appears in the 220−240 nm region and may correspond to a higher extent of structure (disorder to order transition).[40] However, it cannot be directly related to the compaction of IB5 and thus cannot be used to quantify the effects seen in the IMS data set. This outlines the need for complementary methods and the potential role of IMS in structural biology, in particular, for protein complexes displaying polydispersity, heterogeneity, and eventually insolubility.

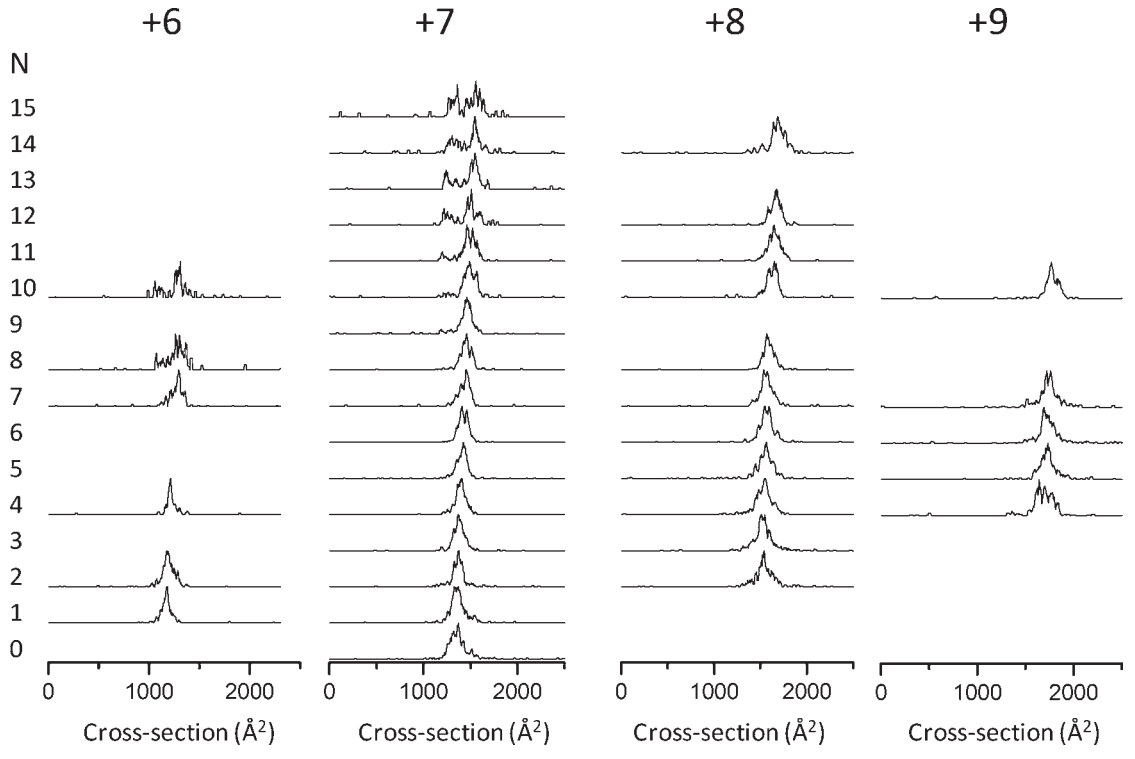

Figure 3. Collision cross section distributions of IB5a·*N* EgCG complexes recorded for charge states 6+, 7+, 8+, and 9+.

dx.doi.org/10.1021/ja200534f |*J. Am. Chem. Soc.* 2011, 133, 7847–7852

Modeling. IMS measurements are usually analyzed by calculating cross sections for unsolvated trial conformations obtained from molecular modeling. However, predicting the structure of noncovalent complexes with hundreds of atoms is clearly still out of reach. We chose to qualitatively interpret the experimental results using a coarse grained force field in which each amino acid and each tannin were replaced by single beads. The force field includes bonds, angles, van der Waals terms between amino acid beads, and a van der Waals term between tannins and amino acids (see Table S1 in the Supporting Information). Either a van der Waals term or a purely repulsive one was used between tannins in order to generate structures where tannins are, respectively, aggregated or separated. We want to outline that the only aim of this simple beads approach is to generate various model structures but that it cannot provide any energetic scale between them or binding information at the atomic level. For our purpose, the most significant parameters are the distance between two beads in the force field, as well as the size of each bead for the collisional cross section calculation. The distance between two amino acid beads was chosen to reflect the average distance between C_α atoms obtained from a sample of structures of IB5 optimized using Amber 99. We then generated structures by a Replica Exchange Monte Carlo simulation algorithm.[41] A total of 20 replicas were used and distributed according to an arithmetic progression in the temperature range 250−600 K. Representative samples of 400 configurations per replica were saved. Their cross sections were calculated using the exact hard sphere model[42] with a radius of 3.5 Å for an amino acid bead and of 7 Å for a tannin. These values were chosen to reproduce the calculated cross section values obtained with an all atom representation for different structures of IB5 and for the calculated cross section of an isolated tannin. Comparison between experimental and calculated cross section values allows the identification of structures that may account for experimental results.

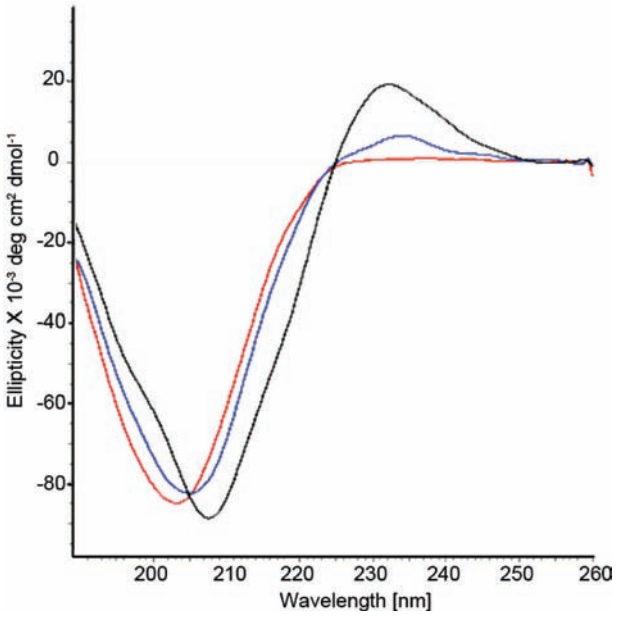

Figure 4. Circular dichroism spectra of IB5 solution (red) and the interaction mixtures 1:N IB5/EgCG (N = 10 (blue) and 40 (black) molar ratio).

Before discussing the simulation results, we want to outline that the model of an organized proline helix leads to much larger collision cross section than any of the two IMS peaks observed. Examples of calculated structures for the naked IB5 protein, 1·9 and 1·14 complexes that are in agreement with the experimental cross section values are shown in Figure 5. The measured cross-section for the bare IB5 corresponds to the open conformation expected for a proline-rich protein and is close to the one deduced from small-angle X-ray scattering (SAXS) measurements in solution.[32] The first family of peaks of 1·9 and 1·14 complexes can be reproduced by calculated structures where the tannins stick separately on the protein (Figure 5b,d). The principal forces driving in-solution association are governed by hydrogen bonding between the carbonyl function of proline residues and the tannin OH groups,[43−45] which leads in solution at low tannin concentration to a binding of a few number of individual tannins as proposed here. Theoretically, each additional tannin induces a significant increase in the collision cross section of the IB5 complex due to the extended geometry of EgCG (Table S2 in the Supporting Information). The comparison of IMS experimental results and simulations suggests that each added tannin induces a slight folding of IB5.

The latter model cannot account for the second peak with an apparent more compact conformation. While juxtaposed tannins show a large calculated collision cross section, IMS measurements on stacks of two and three tannins show that they have close collision cross sections (see the Supporting Information). This is confirmed by simulations performed on three-dimensional stacks of tannins (see Table S2 in the Supporting Information). Therefore, we propose that the second population peaks

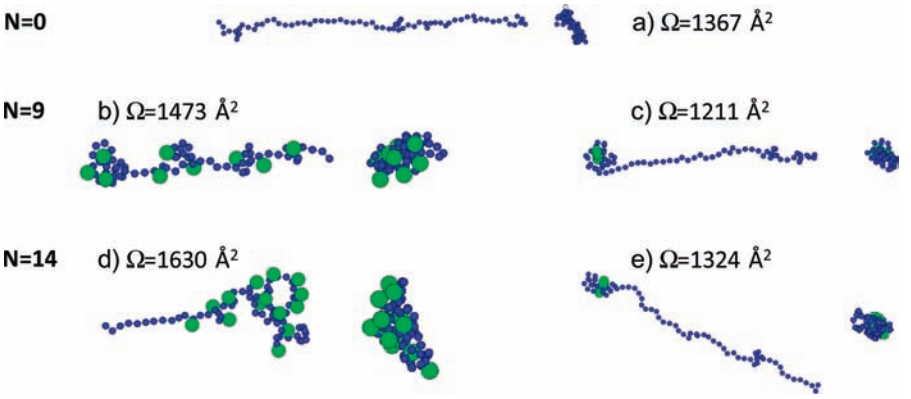

Figure 5. Examples of calculated structures for IB5a (a), IB5a·9 EgCG (b and c), and IB5a·14 EgCG complexes (d and e) which display experimental cross sections in agreement with experimental results (a top and a side view are displayed). In parts b and d, the tannins are dispersed while in parts c and e they are stacked. The blue circles correspond to amino acid beads, while the green ones correspond to tannin beads.

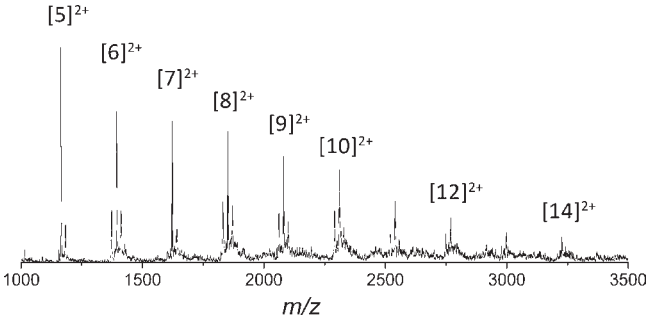

Figure 6. Positive ion mass spectrum of EgCG tannins. The most intense peak for each size corresponds to $[N\ EgCG + 2Na]^{2+}$ species.

characterized by a low cross section correspond to IB5 folded around compact aggregates of tannins. The folding is favored by multiple hydrogen bonds between IB5 and the different hydroxyl groups available on a stack of tannins.[45] This hypothesis is reinforced by the observation of aggregates of tannins when electrospraying a solution of tannins without IB5 (Figure 6), which demonstrates the availability of soluble aggregates of tannins in the experimental solution. These structures may be the first step toward the formation of large colloids of tannins and proteins. Indeed, a common view on tannin−protein complexation and precipitation is that, first, tannins aggregate on proteins. In secondary interactions, protein−tannin complexes self-associate via further hydrogen bonding between tannins acting as linker between several proteins. This triggers the formation of insoluble complexes that precipitate.[25,26,44] This mechanism was particularly well characterized in solution for polyphenol and β-casein interactions,[28] which highlighted the compaction of the protein upon binding to tannins, then aggregation leading to precipitation. Our results show that a similar mechanism involving first a compaction is also probable for salivary proteins. The family of structures with dispersed tannins (less compact) might correlate to the bimodal distributions observed in solution,[25] although they may be here enhanced by coloumbically driven unfolding. Finally, we outline that the broadness of the peaks in the collision cross section shows that each peak does not correspond to a single structure but to a family of structures. These may correspond to different binding sites of tannins on the protein leading to a wide range of conformers. A partial mixing of two complexation pathways (addition of single tannins and addition of an aggregate of tannins) cannot be excluded and may allow a fast binding of numerous tannins, which is in agreement with the biological roles of salivary proteins.

CONCLUSIONS

In summary, IMS was used to get a snapshot of the conformational distribution within a complex mixture of one model of salivary IDP protein bound to its natural target and of its conformational adaptability. The first important result is that a single protein can bind up to 15 tannins. IMS measurements show a transition from extended to more compact structures as the number of tannins bound to the protein increases. We propose that this transition is due to a competition between the binding of individual tannins and the binding of aggregated tannins. Both pathways of complexation coexist at high tannin concentration, which illustrates the capability of IDPs to efficiently bind targets in different manners. In the near future, IMS could be part of integrated approaches, which have to be developed to evolve from a static picture of functional IDPs to a dynamic one, in which several conformations are consistent with various aspects of function.

ASSOCIATED CONTENT

Supporting Information. Chemical structure of EgCG and sequence of IB5; MS/MS spectrum of the IB5a·9 EgCG complex; and cross sections for assemblies of tannins. This material is available free of charge via the Internet at http://pubs.acs.org.

AUTHOR INFORMATION

Corresponding Author
dugourd@lasim.univ-lyon1.fr

ACKNOWLEDGMENT

The authors thank Dr. Véronique Cheynier and Dr. Franck Paté for helpful scientific discussions and Thérèse Marlin for protein purification. Francis Canon was supported by a grant of French Ministry of Research. This work is supported by Grants 07-BLAN-0279 and 05-BLAN-0086 from the French Agence Nationale de la Recherche (A.N.R.).

REFERENCES

(1) Wright, P. E.; Dyson, H. J. *J. Mol. Biol.* **1999**, *293*, 321–331.
(2) Dunker, A. K.; Silman, I.; Uversky, V. N.; Sussman, J. L. *Curr. Opin. Struct. Biol.* **2008**, *18*, 756–764.
(3) Dyson, H. J.; Wright, P. E. *Nat. Rev. Mol. Cell Biol.* **2005**, *6*, 197–208.
(4) Tompa, P. *Trends Biochem. Sci.* **2002**, *27*, 527–533.
(5) Cortese, M. S.; Uversky, V. N.; Dunker, A. K. *Prog. Biophys. Mol. Biol.* **2008**, *98*, 85–106.
(6) Dyson, H. J.; Wright, P. E. . In *Nuclear Magnetic Resonance of Biological Macromolecules, Part B*; Methods in Enzymology, Vol. 339; Academic Press: San Diego, CA, 2001; pp 258−270.
(7) Bernado, P.; Mylonas, E.; Petoukhov, M. V.; Blackledge, M.; Svergun, D. I. *J. Am. Chem. Soc.* **2007**, *129*, 5656–5664.
(8) Svergun, D. I. *Biol. Chem.* **2010**, *391*, 737–743.
(9) Charlton, A. J.; Haslam, E.; Williamson, M. P. *J. Am. Chem. Soc.* **2002**, *124*, 9899–9905.
(10) Edelmann, A.; Lendl, B. *J. Am. Chem. Soc.* **2002**, *124*, 14741–14747.
(11) Bowers, M. T.; Kemper, P. R.; von Helden, G.; van Koppen, P. A. M. *Science* **1993**, *260*, 1446–1451.
(12) Clemmer, D. E.; Jarrold, M. F. *J. Mass Spectrom.* **1997**, *32*, 577–592.
(13) Dugourd, P.; Hudgins, R. R.; Clemmer, D. E.; Jarrold, M. F. *Rev. Sci. Instrum.* **1997**, *68*, 1122–1129.
(14) Clemmer, D. E.; Hudgins, R. R.; Jarrold, M. F. *J. Am. Chem. Soc.* **1995**, *117*, 10141–10142.
(15) Faull, P. A.; Florance, H. V.; Schmidt, C. Q.; Tomczyk, N.; Barlow, P. N.; Hupp, T. R.; Nikolova, P. V.; Barran, P. E. *Int. J. Mass Spectrom.* **2010**, *298*, 99–110.
(16) Politis, A.; Park, A. Y.; Hyung, S. J.; Barsky, D.; Ruotolo, B. T.; Robinson, C. V. *PLoS ONE* **2010**, *5*, 11.
(17) Murray, M. M.; Bernstein, S. L.; Nyugen, V.; Condron, M. M.; Teplow, D. B.; Bowers, M. T. *J. Am. Chem. Soc.* **2009**, *131*, 6316.
(18) Bernstein, S. L.; Dupuis, N. F.; Lazo, N. D.; Wyttenbach, T.; Condron, M. M.; Bitan, G.; Teplow, D. B.; Shea, J. E.; Ruotolo, B. T.; Robinson, C. V.; Bowers, M. T. *Nat. Chem.* **2009**, *1*, 326–331.
(19) Grabenauer, M.; Wyttenbach, T.; Sanghera, N.; Slade, S. E.; Pinheiro, T. J. T.; Scrivens, J. H.; Bowers, M. T. *J. Am. Chem. Soc.* **2010**, *132*, 8816–8818.

(20) Bernstein, S. L.; Liu, D.; Wyttenbach, T.; Bowers, M. T.; Lee, J. C.; Gray, H. B.; Winkler, J. R. *J. Am. Soc. Mass Spectrom.* **2004**, *15*, 1435–1443.
(21) Pascal, C.; Poncet-Legrand, C.; Imberty, A.; Gautier, C.; Sarni-Manchado, P.; Cheynier, V.; Vernhet, A. *J. Agric. Food Chem.* **2007**, *55*, 4895–4901.
(22) Quideau, S.; Deffieux, D.; Douat-Casassus, C.; Pouységu, L. *Angew. Chem., Int. Ed.* **2011**, *50*, 586–621.
(23) Poncet-Legrand, C.; Cabane, B.; Bautista-Ortin, A. B.; Carrillo, S.; Fulcrand, H.; Perez, J.; Vernhet, A. *Biomacromolecules* **2010**, *11*, 2376–2386.
(24) Zanchi, D. e.; Vernhet, A.; Poncet-Legrand, C. l.; Cartalade, D.; Tribet, C.; Schweins, R.; Cabane, B. *Langmuir* **2007**, *23*, 9949–9959.
(25) Charlton, A.; Baxter, N. J.; Khan, M. L.; Moir, A. J. G.; Haslam, E.; Davis, A. P.; Williamson, M. P. *J. Agric. Food Chem.* **2002**, *50*, 1593–1601.
(26) Zanchi, D.; Poulain, C.; Konarev, P.; Tribet, C.; Svergun, D. I. *J. Phys.: Condens. Matter* **2008**, *20*, 4224.
(27) Sarni-Manchado, P.; Canals-Bosch, J.-M.; Mazerolles, G.; Cheynier, V. *J. Agric. Food Chem.* **2008**, *56*, 9563–9569.
(28) Jobstl, E.; O'Connell, J.; Fairclough, J. P. A.; Williamson, M. P. *Biomacromolecules* **2004**, *5*, 942–949.
(29) Vidal, S.; Francis, L.; Noble, A.; Kwiatkowski, M.; Cheynier, V.; Waters, E. *Anal. Chim. Acta* **2004**, *513*, 57–65.
(30) Zucker, W. V. *Am. Nat.* **1983**, *121*, 335–365.
(31) Dunker, A. K.; Oldfield, C. J.; Meng, J.; Romero, P.; Yang, J. Y.; Walton-Chen, J.; Vacic, V.; Obradovic, Z.; Uversky, V. N. *BMC Genomics* **2008**, *16*, 1–26.
(32) Boze, H.; Marlin, T.; Durand, D.; Pérez, J.; Vernhet, A.; Canon, F.; Sarni-Manchado, P.; Cheynier, V.; Cabane, B. *Biophys. J.* **2010**, *99*, 656–665.
(33) Canon, F.; Paté, F.; Meudec, E.; Marlin, T.; Cheynier, V.; Giuliani, A.; Sarni-Manchado, P. *Anal. Bioanal. Chem.* **2009**, *395*, 2535–2545.
(34) Albrieux, F.; Calvo, F.; Chirot, F.; Vorobyev, A.; Tsybin, Y. O.; Lepère, V.; Antoine, R.; Lemoine, J.; Dugourd, P. *J. Phys. Chem. A* **2010**, *114*, 6888–6896.
(35) Albrieux, F.; Antoine, R.; Chirot, F.; Lemoine, J.; Dugourd, P. *Eur. J. Mass Spectrom.* **2010**, *16*, 557–565.
(36) Revercomb, H. E.; Mason, E. A. *Anal. Chem.* **1975**, *47*, 970–983.
(37) Lees, J. G.; Smith, B. R.; Wien, F.; Miles, A. J.; Wallace, B. A. *Anal. Biochem.* **2004**, *332*, 285–289.
(38) Culard, F.; Laine, B.; Sautiere, P.; Maurizot, J. C. *FEBS Lett.* **1993**, *315*, 335–339.
(39) Wyttenbach, T.; von Helden, G.; Bowers, M. T. *Int. J. Mass Spectrom. Ion Processes* **1997**, *165/166*, 377–390.
(40) Receveur-Bréchot, V.; Bourhis, J. M.; Uversky, V. N.; Canard, B.; Longhi, S. *Proteins* **2006**, *62*, 24–45.
(41) Sugita, Y.; Okamoto, Y. *Chem. Phys. Lett.* **1999**, *314*, 141–151.
(42) Shvartsburg, A. A.; Jarrold, M. F. *Chem. Phys. Lett.* **1996**, *261*, 86–91.
(43) Simon, C.; Barathieu, K.; Laguerre, M.; Schmitter, J. M.; Fouquet, E.; Pianet, I.; Dufourc, E. J. *Biochemistry* **2003**, *42*, 10385–10395.
(44) Hagerman, A. E.; Rice, M. E.; Ritchard, N. T. *J. Agric. Food Chem.* **1998**, *46*, 2590–2595.
(45) Canon, F.; Giuliani, A.; Paté, F.; Sarni-Manchado, P. *Anal. Bioanal. Chem.* **2010**, *398*, 815–822.